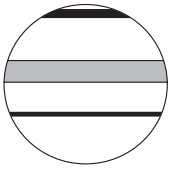

Research Paper

The Holocene
1–11

DOI: 10.1177/09596836231225725
journals.sagepub.com/home/hol
Sage

A speleothem record of hydroclimate variability in northwestern Madagascar during the mid-late Holocene

Berry L Williams,[1] Stephen J Burns,[1] Nick Scroxton,[2] Laurie R Godfrey,[3] Benjamin H Tiger,[4,5] Brian Yellen,[1] Robin R Dawson,[1] Peterson Faina,[6] David McGee[4] and Lovasoa Ranivoharimanana[6]

Abstract

We present a continuous high-resolution precisely dated multiproxy record of hydroclimate variability at Anjohibe cave in northwestern Madagascar using speleothem AB13. The record spans from ~4484 y BP to ~2863 y BP. Stalagmite $\delta^{18}O$, $\delta^{13}C$ and Sr/Ca ratios show very similar changes in hydroclimate. The mechanism controlling Sr/Ca changes, however, from prior calcite precipitation to degree of dolomite dissolution at about 4 ky BP. Our record is also in good agreement with previously published speleothem records from the same area. This agreement and multiproxy consensus indicate that AB13 provides a robust record of hydroclimate variability, including a continuous record of hydroclimate variability across the 4.2 ka event. This 4.2 ka event in Madagascar is marked by two distinct periods of drying between ~3900 y BP to 4300 y BP. A dry 4.2 ka event at this Southern Hemisphere site helps limit possible mechanisms for the event, indicating that a meridional shift to the south in the ITCZ is not responsible for the 4.2 ka event. In addition, the 4.2 ka event does not stand out as a unique dry period in our record. The longest and driest period of the record lasted ~300 years with peak dryness at ~3000 y BP. Our record differs significantly from a speleothem record from Rodrigues Island, located ~1800 km to the east of our study area in Madagascar suggesting different climatological controls on northwest Madagascar and more oceanic sites to the east.

Keywords

Anjohibe, hydroclimate, late-Holocene, Madagascar, mid-Holocene, paleoclimate, rainfall variability, speleothem, Sr/Ca trace element, δ18O and δ13C

Received 14 June 2023; revised manuscript accepted 18 December 2023

Introduction

Climate change over the last century has greatly impacted global precipitation patterns, as well as mean and seasonal temperatures. Many uncertainties about future climate variability remain, particularly in the Southern Hemisphere where high-resolution climate data are regionally limited (Marcott et al., 2013; Voarintsoa et al., 2021; Wanner et al., 2015). As atmospheric CO_2 continues to increase and global climate extremes become increasingly frequent, generating high-resolution, precisely dated records of past climate is key to identifying the mechanisms responsible for its variability. Madagascar, the world's fourth largest island, lies approximately 400 km east of the African continent, in the southwestern Indian Ocean (Figure 1). Over 70% of the population falls below the poverty line and approximately 60% of the population depend on subsistence agriculture without irrigation systems, making them extremely sensitive to variability in local precipitation (Data from International Fund for Agricultural Development ifad.org; Harvey et al., 2014; Madagascar. LandLinks, 2020).

Speleothems, such as stalagmites, contain multiple geochemical climate proxies and have the potential to yield very high resolution, well-dated reconstructions of past changes in hydroclimate. Such records may be used to infer the nature and causes of hydroclimate variability at various timescales. Here, we present a precisely dated multi-proxy record from ~4480 to 2860 years before present (y BP) from stalagmite AB13, which was collected in 2019 from a cave called Anjohibe ("big cave" in Malagasy) in northwestern Madagascar. Oxygen and carbon stable isotopes and Sr/Ca ratios provide multi-proxy hydroclimate records for the region with an average time resolution of less than 3 years. The data include the first continuous time series of climate across the

[1]Department of Earth Geographic and Climate Sciences, University of Massachusetts Amherst, USA
[2]Irish Climate and Analysis Research Units, Department of Geography, Maynooth University, Ireland
[3]Department of Anthropology, University of Massachusetts Amherst, USA
[4]Department of Earth, Atmospheric, and Planetary Sciences, Massachusetts Institute of Technology, USA
[5]Department of Geology and Geophysics, Woods Hole Oceanographic Institution, USA
[6]Mention Bassins Sédimentaires, Évolution, Conservation, Faculté des Sciences, Université D'Antananarivo, Madagascar

Peterson Faina is currently affiliated to OBT Lab, Lamont-Doherty Earth Observatory, The Climate School, Columbia University, New York, NY, USA.

Corresponding author:
Berry L Williams, Department of Earth Geographic and Climate Sciences, University of Massachusetts Amherst, 627 N. Pleasant St, Amherst, MA 01003, USA.
Email: berrylwilliams888@gmail.com

4.2 ka event from Madagascar, providing a detailed Southern Hemisphere record of the 4.2 ka event in the tropical Indian Ocean. Thus, our data provide an important additional record of the 4.2 ka event in the tropics, where the nature and spatial extent of the event have not been established. We use this record to consider possible forcing mechanisms for the 4.2 ka event and place the structure and amplitude of 4.2 ka variability within the context of overall decadal-scale hydroclimate variability in the mid- to late-Holocene. We test the validity of our record through comparison with existing, lower-resolution records from the study area. We also investigate the soundness of using Holocene hydroclimate records from Rodrigues Island (Li et al., 2018) to infer climate variations on Madagascar because this record has been applied to studies of possible ties between climate and megafaunal populations on Madagascar (Li et al., 2020).

Modern and recent paleoclimate of Madagascar

Madagascar extends from 12° S to 26° S in the southwest Indian Ocean (Jury et al., 1995; Worlddata.info) (Figure 1). The climate varies widely with regional rainfall gradients from east to west and from north to south (Dewar and Richard, 2007; Jury, 2003). Easterly trade winds generate orogenic rainfall year-round to the east of the north-south oriented central highlands, with a rain shadow to the west of the mountains that causes a decrease in precipitation westward (Jury et al., 1995). West of the mountains, the latitudinal position of the tropical rain belt and Indian Ocean sea surface temperatures primarily control the highly seasonal climate (Jury et al., 1995). The northwest region of the island, where Anjohibe is located, experiences a warmer rainy season with temperatures averaging about 27°C (November to April) and a slightly cooler dry season with temperature averaging about 25°C (May to October). Annual rainfall varies between ~1160 and 1600 mm above Anjohibe cave system (Raveloson et al., 2018; Voarintsoa et al., 2021) and typically >70% occurs during the austral summer (DJF) with >90% occurring between November and March (Data from Climate-data.org) (Figure 3).

The annual rainfall cycle is controlled somewhat indirectly by seasonal migration of the ITCZ. The mountains of eastern Madagascar block the strong summer easterlies (Barimalala et al., 2018) from crossing the island. As sea surface temperatures warm, low pressure forms in the Mozambique Channel and over western Madagascar (Barimalala et al., 2020). The northeasterlies north of the island curve around to become northwesterlies and bring moisture to much of the western side of Madagascar. The tropical rainfall belt migrates to 20°S in austral summer, following the center of convergence rather than peak SSTs (Koseki and Bhatt, 2018), and is almost discontinuous from the tropical rainfall belt to the east.

On interannual and longer timescales the controls on rainfall variability are not clear. In the broader region of the western Indian Ocean the Indian Ocean Dipole and resultant SST changes are thought to be important with warmer SSTs associated with positive phases of the IOD resulting in increased rainfall. An analysis by Scroxton et al. (2017) showed no correlation between monthly SST anomalies and monthly rainfall in northwestern Madagascar, except in December. IOD associated variability of SSTs in the west Indian Ocean typically occurs before the Madagascan monsoon season between December and March (Schott and McCreary, 2001). At longer timescales, however, rainfall variability does appear to respond to variability in SSTs and both zonal and meridional atmospheric circulation (Scroxton et al., 2017, 2019; Voarintsoa et al., 2019; Zinke et al., 2004).

Until the past half dozen years information about Holocene past climate in Madagascar came primarily from studies of lacustrine sediments. These records, however, are generally quite low resolution with relatively poor age control (Burney, 1987; Burney et al., 2003; Gasse and Van Campo, 1998, 2001; Matsumoto and Burney, 1994; Vallet-Coulomb et al., 2006) and provide no information about millennial-scale variability. In recent years, a number of paleoclimate records have been published using mainly Malagasy speleothems but also lacustrine sediments (Teixeira et al., 2021), many of which provide higher resolution, better dated records than previously available. The majority of the speleothem records are Holocene and come from caves in northwestern Madagascar (Brook et al., 1999; Burns et al., 2016; Duan et al., 2021; Scroxton et al., 2017, 2023a, 2023b; Voarintsoa et al., 2017, 2019; Wang et al., 2019). Voarintsoa et al. (2017) and Wang et al. (2019) published studies investigating climate in northwestern Madagascar throughout much of the Holocene. Voarintsoa

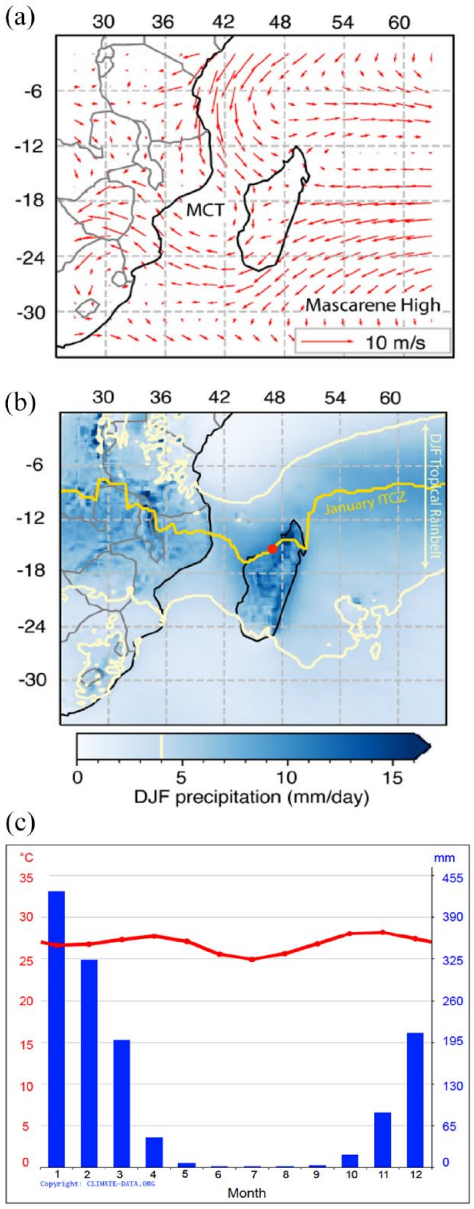

Figure 1. (a) ERA5 850 h Pa January wind direction and strength across southeast Africa, Madagascar (12°S to26°E latitude) and Mascarene Islands (Hersbach et al., 2019). (b) Anjohibe Cave location (15.53°S, 46.88°E) in North Western Madagascar indicated with red dot. Blue gradient indicates austral summer (December, January, and February) mean rainfall, dark yellow line tracks approximate summer position of the ITCZ and the light yellow lines indicate northern and southern boundaries of the rain belt (Adaptation of Ingram and Dawson 2005; Hersbach et al. 2020). (c) Average weather by month in Mahajanga Province from 1991 – 2021. Red line indicates the mean temperatures (Climate-Data.org n.d.).

et al. (2017) suggest the occurrence of three discrete intervals, wet at ~9800–7800 y BP, dry at ~7800–1600 y BP, and wet from ~1600 year BP to present. These wet intervals were primarily attributed to southward migration of the ITCZ, though no mechanism for forcing the ITCZ south was identified. Wang et al. (2019) define six distinct Holocene climate periods with the wettest interval from ~ 9100 to 7500 y BP. Overall, conditions became less variable and drier through the Holocene. Several of the northwest Madagascar speleothem records have also provided information on the timing and structure of the well-documented early Holocene "8.2 ka event" (Duan et al., 2021; Voarintsoa et al., 2017, 2019). In Madagascar the 8.2 ka event is marked by two distinct wet intervals each lasting about 100 years (Duan et al., 2021; Voarintsoa et al., 2019) though the timing of the intervals varies somewhat between records. This wet interval contrasts with a dry 8.2 ka event in the Northern Hemisphere generally and in the northern Indian Ocean region in particular suggesting a southward shift in mean ITCZ globally and regionally (e.g. Cheng et al., 2009).

Approximately 1800 km east of Madagascar on Rodrigues Island, two stalagmite samples record local hydroclimate from ~6000 to 3000 y BP and indicate a somewhat different climate pattern (Li et al., 2018). Records constructed from the $\delta^{18}O$ values of the speleothems do not show any significant long-term climate anomalies from ~6000 to 4000 y BP, rather, they show consistent decadal to multi-decadal scale wet/dry fluctuations across this timespan (with perhaps a very slight overall drying trend from ~5000–3700 y BP). The most notable excursion in the records suggests a multi-centennial drought beginning at ~3900 y BP.

Materials and methods

One of the larger cave systems in the Indian Ocean, Anjohibe, consists of more than 5 km of mapped passages and more than 13 entrances (Brook et al., 1999; Middleton and Middleton, 2003; Rogers et al., 2000). The cave, formed in the Eocene Narinda Karst, is composed of limestone with varying amounts of dolomite (Gunn, 2004). The thickness of carbonate rock above the cave ranges from ~5 m to ~15 m. On a seasonal and diurnal scale, the cave's atmosphere is highly responsive to climatic variability in the surrounding environment (Voarintsoa et al., 2021). Relative humidity (RH) and pCO_2 of the cave reflect local seasonality. During the austral winter, when conditions are dry, the interior of Anjohibe has a lower RH (~63% mean RH) and pCO_2 (~450 ppm). In contrast, during the wet summer months, the cave interior experiences higher RH (~76.5% mean RH) and pCO_2 (~500–600 ppm) (Voarintsoa et al., 2021). Stalagmite AB13 is approximately 30 cm tall and 9.5 cm in diameter; it was collected from Anjohibe in October 2019. The stalagmite was cut in half along the vertical axis and polished (Supplemental Figure 1). The polished surface shows regular mm-scale laminae composed of acicular crystals oriented parallel to the growth axis, a morphology typical of aragonite, with the exceptions of two ~1 cm white, dense microcrystalline layers.

To confirm sample mineralogy, 12 samples, collected every 2.5–4 cm along the growth axis of the stalagmite and including the two dense white layers were analyzed for mineral composition at the Department of Geosciences, Smith College by X-ray diffraction (XRD) using a Rigaku SmartLab SE Diffraction System.

A chronology of AB13 was developed using 14 U-Th dates. Uranium-series dating was done at the Paleoclimate and Geochronology Laboratory at the Massachusetts Institute of Technology (MIT). Subsamples weighing ~200 mg each were drilled and collected every 2–3 cm using a vertical micromill. Samples were combined with a ^{229}Th-^{233}U-^{236}U tracer, digested and purified via iron coprecipitation and ion exchange chromatography. U and Th were analyzed on separate aliquots using a Nu Plasma II-ES multi-collector ICP-MS equipped with a CETAC Aridus II desolvating nebulizer. U-Th ages were calculated using the half-lives of Cheng et al. (2013) and Jaffey et al. (1971) and an initial $^{230}Th/^{232}Th$ ratio of 4.4 ± 2.2 ppm atomic. Ages for this stalagmite are reported as y BP, with present defined as calendar year 1950. Individual date errors range from ± 21–47 years with an average for all subsamples of approximately ± 32 years. We applied a Monte Carlo simulation using Copra software (Breitenbach et al., 2012) in Matlab to construct the age model for AB13 (Figure 2). Age model interpolated dates were then used for growth rate estimates (data were separated into 50-year bins to calculate average growth rates).

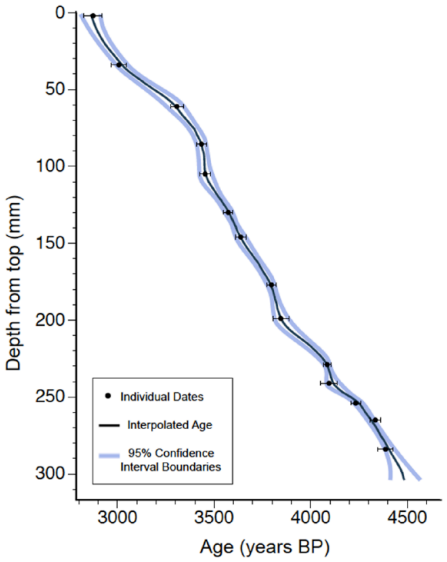

Figure 2. Age model for stalagmite AB13. Black line represents interpolated median ages between individually datedsubsamples, black dots indicate individual dates, and blue highlight indicates 95% CI low and high boundaries. (COPRA source code available at https://tocsy.pik-potsdam.de/copra.php).

A total of 608 oxygen and carbon isotope analyses of AB13 were performed in the Stable Isotope Laboratory at the University of Massachusetts Amherst. Subsamples were taken at 0.5 mm intervals along the center of the growth axis. Isotope ratios were measured using an online Thermo Scientific Gas Bench II carbonate preparation system connected to a Thermo Scientific Delta V Advantage isotope ratio mass spectrometer. Standard material reproducibility is greater than ±0.08‰ for both $\delta^{18}O$ and $\delta^{13}C$. Results are reported in standard δ notation relative to the VPDB standard.

Trace elements were measured using core-scanning micro-X-ray fluorescence (CS-μXRF). Sr/Ca ratios were measured every 0.5 mm using a Cox Analytical System ITRAX core scanner at the University of Massachusetts Amherst. AB13 was analyzed in three runs to ensure alignment of the x-ray beam with the central growth axis of the stalagmite. Samples were run with a molybdenum tube at 50 kV and 45 mA following the procedure outlined by Scroxton et al. (2018).

To determine whether climate cyclicity was present in the time series, wavelet spectral analysis and a power spectrum of the oxygen stable isotope time series were done. Wavelet Spectral Analysis of the stable isotope time series was completed using R package "biwavelet" (Gouhier et al., 2021; Liu et al., 2007; Torrence and Compo, 1998). The time series was interpolated and detrended before wavelet analysis. Power spectrum plots were generated with Python, using the Lomb-Scargle method, thus the data were not interpolated. Prior to spectral analysis, the data were detrended for any linear trend and the mean was removed. A

hamming window with 50% overlap was used with five windows along the data. The spectrum was run using 1000 AR(1)s and 90%, 95%, and 99% significance limits calculated.

Results

Age model

The age model shows that AB13 grew over a ~1620 years period from 4484 y BP to 2863 y BP (Table 1). Mean growth rate for stalagmite AB13 is ~0.31 mm/year. The fastest growth rates occurred at ~4110–4060 y BP (~0.33 mm/year), from ~3860 to 3760 y BP (~0.37 mm/year), and from ~3460 to 3410 y BP (~1.26 mm/year). The slowest growth rates occurred from ~4210 to 4160 y BP (~0.08 mm/year), from ~3960 to 3910, and from ~3260 to 3065 y BP.

Mineralogy

The XRD results confirm visual, crystal morphological indicators of mineralogy. AB13 is composed almost entirely of aragonite interrupted by two thin (<1 cm) layers of calcite. No calcite was detected outside of the two dense, white layers.

Stable isotopes

The 608 subsamples taken along the growth axis of stalagmite AB13 were analyzed for $\delta^{18}O$ and $\delta^{13}C$ (Figure 3). The average temporal resolution of the record is 2.7 years, with a maximum of ~ 0.1 years and a minimum of ~ 6.8 years. Oxygen isotope values range from a minimum of −6.73‰ to a maximum of −2.10‰ with a mean value of −3.88‰ (Figure 3). From ~4485 to 3480 y BP, values range from ~3‰ to 5‰, with a mean value of 3.86‰. Within this time, there are periods of relatively enriched values of −2‰ to −3‰. At ~4460 years there is a 200 year trend of increasing values leading to the first interval of enriched values at ~4280–4180 y BP. Values also become enriched at ~4055–4025 y BP, and again between ~4000 and 3960 y BP. At ~ 3475–3450 y BP, the interval associated with the calcite layers, values become significantly more depleted (between −5.53‰ and − 6.71‰). The most prominent feature occurs immediately after this negative excursion. Isotope values become increasingly enriched in ^{18}O by ~3‰ from ~ 3450 to 3200 y BP, leading into a several hundred-year interval with the most enriched isotope values in the record. From ~3120 to 2990 y BP, $\delta^{18}O$ values remained relatively enriched, between ~ −2‰ and −3‰. Between 2995 y BP and 2860 y BP, values range from −4.67‰ to −3.32‰.

The $\delta^{13}C$ values show a very similar variation over time to $\delta^{18}O$ but vary more widely, from −10.13‰ and −1.81 ‰, with a mean of −6.22‰ (Figure 3). For most of the record, from ~4485 to 3480 y BP, values fall within a narrower range, from −8.01‰ and −4.03‰. However, $\delta^{13}C$ values become relatively enriched, falling between ~ −4.0‰ to −5.0‰, at ~4280–4190 y BP, at ~4055 y BP, and from ~4000 to 3950 y BP. Between ~3470 and 3450 years BP there are extremely negative values (maximum −6.43‰; minimum −10.13‰; mean 8.88‰) corresponding to the calcite layers. After the brief period of depleted values, there is a ~300-year trend of increasing $\delta^{13}C$ values. The highest $\delta^{13}C$ values in the record occur between ~3200 and 3000 y BP with mean values of −3.10‰ (minimum −4.47‰; maximum 1.18‰). Throughout the interval near the top of AB13, from ~2990 to 2860 y BP, the values range from a maximum of −3.91‰ to a minimum −7.41‰ with a mean of −6.35‰.

Trace elements

Sr/Ca ratios are also shown in Figure 3. Mean temporal resolution of Sr/Ca is ~ 3.1 years. The Sr/Ca data from the two thin intervals

Table 1. U-Th dating results for stalagmite AB13.

Sample ID	Depth (mm)	^{238}U (ng/n)[a]	± (2σ)	^{232}Th (pg/g)[a]	± (2σ)	$\delta^{234}U$ (per mil)[b]	± (2σ)	$^{230}Th/^{238}U$ activity	± (2σ)	$^{230}Th/^{232}Th$ (ppm atomic)	± (2σ)	Age (yr) (uncorr)[c]	± (2σ)	Age (yr) (corr)[d]	± (2σ)	$\delta^{234}U$ (per mil)[e]	± (2σ)	Age (yr BP) (corr)[f]	± (2σ)
Bottom	284	1827.43	36.55	287.84	9.09	3.74	2.22	0.04025	0.00033	4056.92	104.24	4462	39	4458	39	3.79	2.25	4387	39
AB13-1A	2	1552.65	31.05	3131.45	62.90	6.23	2.90	0.02735	0.00031	215.28	2.46	3005	36	2944	47	6.28	2.93	2873	47
AB13-1B	61	1344.27	26.89	1120.45	22.77	4.54	2.19	0.03087	0.00027	587.96	5.46	3403	31	3378	34	4.59	2.21	3307	34
AB13-1C	105	1892.89	37.86	173.64	5.83	6.11	2.30	0.03202	0.00024	5542.71	154.82	3527	29	3524	29	6.17	2.32	3453	29
AB13-1D	146	1650.18	33.00	210.29	6.22	2.65	2.08	0.03357	0.00024	4182.54	95.61	3713	28	3709	28	2.68	2.10	3638	28
AB13-1E	199	2014.32	40.29	130.91	5.42	3.99	1.85	0.03544	0.00036	8657.41	325.68	3918	41	3916	41	4.03	1.88	3845	41
AB13-1F	241	1755.69	35.11	148.47	5.42	5.30	1.88	0.03771	0.00037	7080.46	226.65	4169	43	4167	43	5.37	1.90	4095	43
AB13-2A	34	1450.41	29.01	2879.61	59.09	7.23	2.00	0.02852	0.00023	228.05	2.09	3132	27	3072	40	7.29	2.02	3007	40
AB13-2B	85.5	2061.21	41.24	1957.98	40.71	6.51	1.94	0.03204	0.00018	535.52	4.13	3528	21	3499	25	6.58	1.96	3434	26
AB13-2C	130	1591.04	31.82	231.10	13.39	6.92	1.82	0.03308	0.00020	3615.55	197.78	3642	24	3638	24	6.99	1.83	3573	24
AB13-2D	177	1570.60	31.42	110.94	11.31	5.30	2.18	0.03499	0.00019	7864.82	787.54	3863	23	3861	23	5.36	2.20	3796	23
AB13-2E	229	2020.16	40.41	178.65	13.54	5.54	2.10	0.03758	0.00017	6746.20	494.04	4153	21	4150	21	5.60	2.13	4085	21
AB13-2F	265	1560.77	31.22	958.86	22.45	5.83	2.24	0.03994	0.00022	1032.30	13.64	4419	27	4400	28	5.91	2.27	4335	28
AB13-254	254	1601.27	32.03	663.80	13.35	6.24	2.08	0.03896	0.00021	1492.24	8.25	4310	26	4298	26	6.32	2.11	4233	26

[a]Reported errors for ^{238}U and ^{232}Th concentrations are estimated to be ±1% due to uncertainties in spike concentration; analytical uncertainties are smaller

[b]$\delta^{234}U = ([^{234}U/^{238}U]_{activity}-1)\times 1000$

[c]$[^{230}Th/^{238}U]_{activity} = 1 - e^{-\lambda_{230}T} + (\delta^{234}U_{measured}/1000)[\lambda_{230}/(\lambda_{230}-\lambda_{234})](1 - e^{-(\lambda_{230}-\lambda_{234})T})$, where T is the age. "Uncorrected" indicates that no correction has been made for initial ^{230}Th

[d]Ages are corrected for detrital ^{230}Th assuming an initial $^{230}Th/^{232}Th$ of $(4.4 \pm 2.2)\times 10^{-6}$.

[e]$\delta^{234}U_{initial}$ corrected was calculated based on ^{230}Th age (T), that is, $\delta^{234}U_{initial} = \delta^{234}U_{measured} \times e^{\lambda_{234}*T}$, and T is corrected age.

[f]B.P. stands for "Before Present" where the "Present" is defined as the 1 January 1950 C.E.

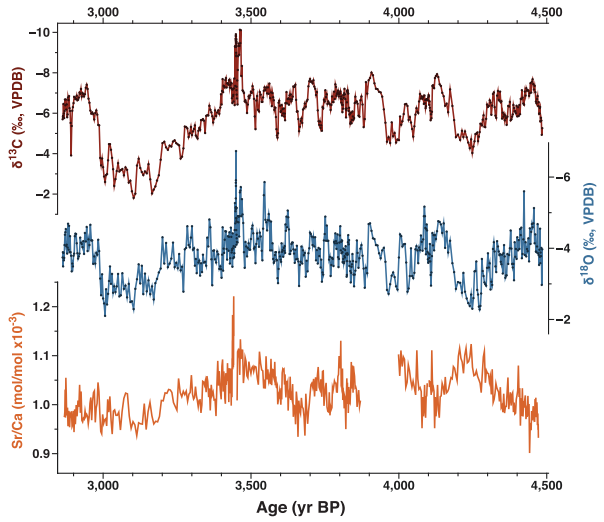

Figure 3. Time series of stable isotope and trace element analyses for stalagmite AB13. Records show variations in $\delta^{13}C$ (‰) (red), $\delta^{18}O$ (‰) (blue), Sr/Ca (mol/mol x10-3) (orange) during the mid-late Holocene (~4,485 to ~2,860 years BP).

of calcite were removed from the figure because the mineral structure of calcite incorporates strontium less readily than aragonite, resulting in Sr/Ca values roughly three times lower than those for aragonite. Removing the calcite data more clearly shows the trends in the aragonitic portions of the speleothem. A gap of approximately 200 years, from 4000 y BP to 3800 y BP, appears in the record because of edge effect on the XRF data where the sample was broken into two pieces. From the period at the start of the record to ~4220 y BP, the Sr/Ca record shows a trend of increasing values. The aragonitic intervals with the highest strontium concentrations occur at ~3948–3905 y BP, 3806 y BP, and 3442–3437 years BP. The lowest concentrations occur at ~4454–4447 y BP, 4385 y BP and 3895–3881 y BP.

Spectral analysis

The $\delta^{18}O$ time series clearly contain variability at multi-decadal timescales. For example the wavelet analysis indicates some significant cycles in the 30–60 year band and the power spectrum shows the presence of a number of frequencies in the 10–20 year band that are statistically significant (Supplemental Figures 2 and 3). The wavelet analysis, however, shows that none of the decadal variability is present over more than a timespan of a few decades and no coherent decadal or centennial scale cycles are detectable across the record. The very short periods where cycles are present suggests there is not an interpretable external or internal forcing this variability that is other than stochastic. These results are, therefore, not discussed further.

Discussion

Oxygen and carbon isotopes as paleoclimate proxies

In Madagascar, as for many other tropical and monsoonal climates, the amount effect (Dansgaard, 1964) is interpreted to be the dominant control on $\delta^{18}O$ values of meteoric precipitation (Burns et al., 2016; Fleitmann et al., 2003; Lachniet, 2009; McDermott, 2004; Scroxton et al., 2017; Voarintsoa et al., 2017; Wang et al., 2001). The amount effect results in rain with comparatively higher $\delta^{18}O$ values during light precipitation events and lower $\delta^{18}O$ values in heavy precipitation events (Bowen et al., 2019). No relevant modern data for directly examining the relationship between rainfall amount and $\delta^{18}O$ exist for the study area. The closest location with extensive measurements of rainfall isotopes is Antananarivo, in central Madagascar, where an amount effect is observed (Voarintsoa, 2021). We recognize that the processes governing the amount effect are complex (e.g. Konecky et al., 2019), with moisture transport pathway, sub-cloudbase microphysics and cloud type also playing important roles in determining the isotopic composition of rainfall. From a paleoclimate perspective, possible past variations in these factors cannot explicitly be accounted for. Nevertheless, a number of factors that apply to Anjohibe suggest it is well situated for an amount effect to be the primary driver of changes in $\delta^{18}O$. First, the rainfall in the area has single moisture source, the western tropical Indian Ocean (Scroxton et al., 2017). Moisture source changes, often a confounding influence on speleothem $\delta^{18}O$, are unlikely to be a factor. Second, Anjohibe is in a coastal location very close to the moisture source. Empirical and modeling studies of the amount effect show that it is better expressed for coastal locations than in continental interiors (Araguás-Araguás et al., 2000; Kurita et al., 2009). In addition, Duan et al. (2021), using the IsoGSM model (Yoshimura et al., 2008), showed a strong and statistically significant correlation ($r=-0.4$, $p<0.1$) between rainfall at the Anjohibe cave site and precipitation amount at the site and in a broad region of the surrounding tropical Indian Ocean. Thus, we interpret an increase (decrease) in $\delta^{18}O$ values as generally indicating drier (wetter) paleoclimate conditions. Because other factors may nevertheless contribute to $\delta^{18}O$ variability, we utilize additional possible hydroclimate proxies, $\delta^{13}C$ and speleothem Sr/Ca, in conjunction with $\delta^{18}O$ and compare our record to existing, lower -resolution speleothem records from the same cave.

Carbon isotopes from speleothem calcite are often more complex than oxygen isotopes, with values typically reflecting some combination of climatic controls and local soil-karst processes. The primary controls are temperature, vegetation cover, and precipitation amount (Fohlmeister et al., 2020; McDermott, 2004). Many of these controls are also closely linked to climate, which often allow $\delta^{13}C$ values to also be interpreted as a proxy for hydroclimate. Wetter climate conditions generally result in more vegetation, and thus, more plant respired CO_2, and more decay of organic matter, both of which are isotopically depleted. Consequently, $\delta^{13}C$ values often have a negative relationship with precipitation, whereby wet and dry are reflected by more negative values and less negative values, respectively (Fohlmeister et al., 2020).

Carbon isotopes may also reflect the type of vegetation, specifically the photosynthetic pathway. $\delta^{13}C$ values have been interpreted in terms of the changes in the C_3/C_4 ratio in the flora above Anjohibe related to the surface ecosystem (Burns et al., 2016). The ratios reflect the difference in isotopic fractionation that occurs in the photosynthetic pathways of C_3 plants such as woody taxa and C_4 plants such as open habitat grasses. The former are generally favored in wetter conditions and are associated with more isotopically depleted values; while C_4 grasses are reflected by more enriched values and tend to grow during drier periods. In addition to these primary drivers, $\delta^{13}C$ values may be subject to fractionation effects that occur during the degassing of CO_2 in the epikarst (Fairchild et al., 2006) during prior calcite (or aragonite) precipitation, again, where wetter conditions are associated with more depleted values.

In this study, we interpret variations in the $\delta^{13}C$ to be primarily hydroclimate driven with changes in the percentage of C_4 grasses and prior carbonate precipitation (discussed below) possible additional factors influencing speleothem $\delta^{13}C$. For all of these processes, increases (decreases) in $\delta^{13}C$ values signify drier (wetter) conditions as has also been suggested in previous Anjohibe studies (Burns et al., 2016; Voarintsoa et al., 2017, 2019).

Sr/Ca as paleoclimate proxy in Anjohibe

Speleothem Sr/Ca is frequently used as additional climate indicator in speleothem paleoclimate studies (Fairchild et al., 2006;

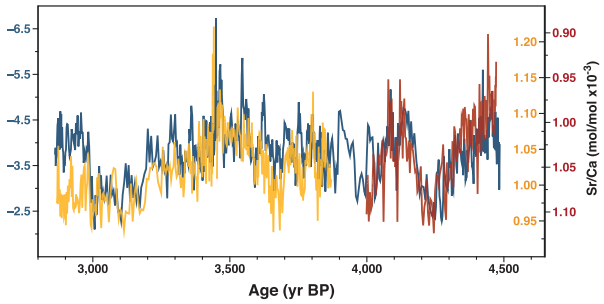

Figure 4. Comparison of AB13 $\delta^{18}O$ and Sr/Ca time series. Note that the scale for the Sr/Ca data reverses from increasing downwards for the older portion of the record (4.6 ky BP to 4.0 kyBP), red in color, to increasing upwards for the remainder of the record, orange/yellow in color.

Scroxton et al., 2017, 2018). The primary control on speleothem Sr/Ca is most often considered to be the extent of calcite precipitated in the karst system prior to dripwater reaching actively growing stalagmites (Fohlmeister et al., 2020). The extent of prior calcite precipitation (PCP) is in turn controlled by the residence time of groundwater in the karst system, with drier conditions associated with a longer residence time, more extensive PCP and higher Sr/Ca in cave drip waters and speleothems. Whether and how this interpretation applies to Anjohibe requires considering at least one additional important actor: the bedrock is a mixture of limestone ($CaCO_3$) and dolostone ($CaMg(CO_3)_2$). Marine dolostones typically contain between 50 and 100 ppm Sr whereas marine limestones typically have on the order of 1000 ppm Sr. Thus, the extent of dolomite versus calcite dissolution in the epikarst could have a strong impact on the drip water Sr/Ca ratios.

Figure 4 shows the Sr/Ca and $\delta^{18}O$ time series plotted together. In this figure the scale for the Sr/Ca time series changes sign at approximately 4 ky BP. For the period from 4.6 ky BP to 4 ky BP Sr/Ca are shown with the scale inverted (values increase downward) and from 4 ky BP to the end of the time series the scale has values increasing upward. The data are shown in this form because we suggest that a change in the mechanism controlling speleothem Sr/Ca occurred at ~4 ky BP. For the older part of the record Sr/Ca and $\delta^{18}O$ are strongly and positively correlated. We interpret this correlation to be the result of changing residence time of water in the epikarst, with PCP being the dominant mechanism controlling drip water and speleothem Sr/Ca. As noted above, drier conditions are associated with decreased rainfall, a longer groundwater residence time, and increased Sr/Ca. Dry conditions also result in less negative rainfall $\delta^{18}O$ values and speleothem $\delta^{18}O$ values, explaining the positive correlation between Sr/Ca and $\delta^{18}O$ for this interval.

From ~4 ky BP to the end of speleothem growth, Sr/Ca is strongly anticorrelated with $\delta^{18}O$ and $\delta^{13}C$. The observed anticorrelations indicates that PCP is very unlikely to be the mechanism controlling speleothem Sr/Ca over this time. One possible alternative is that prior aragonite precipitation (PAP) in the epikarst drives changes in dripwater Sr/Ca (Scroxton et al., 2017; Wassenburg et al., 2016). The D_{Sr} for aragonite is greater than one and, therefore, different degrees of PAP should lead to an anticorrelation between speleothem Sr/Ca and isotopic indicators of rainfall, as we observe. Two problems with this explanation arise, however. First, the great majority of experimental studies suggest a D_{Sr} for aragonite between 1.0 and 1.1 at low temperatures (Dietzel et al., 2004; Gaetani and Cohen, 2006; Giri et al., 2018; Kinsman and Holland, 1969; Mucci et al., 1989). A D_{Sr} close to 1 means that even quite large changes in the extent of PAP result in very minor changes to fluid Sr/Ca values.

Wassenburg et al. (2016), in a study of speleothems, suggested a larger value for D_{Sr} in aragonite of 1.38. Using this value in a simple Rayleigh model of PAP shows that PAP can account for the range of variability in Sr/Ca observed, but only with a very large range of total Ca removal to precipitating aragonite, 0%–70%, which seems unlikely. In addition, PCP increases fluid Sr/Ca whereas PAP decreases fluid Sr/Ca. A change in controlling mechanism from PCP to PAP should lead to a stepped change in speleothem Sr/Ca from higher to lower values at the transition in mechanisms. Figure 4 shows little change in average Sr/Ca values before and after 4 ky BP. Thus, we do not think that PAP can explain the observed changes in Sr/Ca after 4 ky BP.

Instead, we propose that differential dissolution of dolomite and calcite in the overlying epikarst, which is a mixture of both minerals, can explain the anticorrelation. The speleothem $\delta^{18}O$ values are still dominated by an amount effect, and Sr/Ca is still controlled by residence time, but longer (shorter) residence times result in greater (lesser) relative amounts of dolomite dissolution. Because marine dolomite almost invariably has much lower Sr/Ca ratios than marine calcite, greater relative dolomite dissolution will result in a lower speleothem Sr/Ca value. Changes in the relative amounts of dolomite versus calcite dissolution can be explained by the much slower rates of dolomite dissolution compared to calcite at near equilibrium conditions. Overall, we propose that periods of decreased rainfall will be associated with less negative $\delta^{18}O$, longer karst water residence times, greater differential dolomite dissolution, lower speleothem Sr/Ca and a strong observed negative correlation between Sr/Ca and $\delta^{18}O$, as observed.

The above discussion leads to the obvious question of why the mechanism controlling Sr/Ca changed at about 4 ky BP? No clear shift in mean $\delta^{18}O$ values occurs at this time, suggesting a shift in climate was not the cause, though the change in Sr/Ca mechanism did take place after a relatively prolonged dry period. A possible explanation is that this dry period resulted in a changed groundwater flow path, perhaps to one with more mixed mineralogies. Regardless, the close correspondence between speleothem Sr/Ca and $\delta^{18}O$, however, is a strong indicator that AB13 is a robust recorder of climate variability over the period of its deposition.

Northwest Madagascar paleoclimate reconstruction

The stable isotope records and Sr/Ca data produced from stalagmite AB13 reveals that for much of the ~1620 years period covered by this stalagmite, the region experienced several multidecadal wet – dry climate oscillations with no distinct long-term trends. Beginning around 4460 y BP, the region experienced ~200 years of steadily decreasing precipitation followed by a ~100 years period of relatively dry conditions. Peak dryness of the two intervals occurred at ~4275 and ~4250 y BP. A return to relatively wet conditions occurred at ~4180 y BP. At ~4055 y BP, a second interval consisting of several dry periods began. This dry period is interrupted by three intervals of increased rainfall. From ~4025 to 4000 y BP, the region experienced a relatively large increase in precipitation, with conditions returning to almost pre-drought conditions. And finally, toward the end of the drought from ~3985 to 3975 y BP climate became slightly wetter (Figure 3). These two arid intervals fall within the window of previously dated 4.2 ka event (Scroxton et al., 2023b), which is typically reported to have occurred between 4200 and 3900 y BP. We discuss this interval in detail below.

From ~3950 to 3475 y BP, the region experienced generally wet conditions. The widest range in climate variability recorded by stalagmite AB13 is observed in the upper portion of the record. The sharp decrease in $\delta^{18}O$ values suggests that during the interval associated with calcite layers, from ~3475 to 3450 y BP, NW Madagascar experienced extremely wet conditions. Immediately following this wet interval, the climate underwent nearly 300 years of increasing aridity, which culminated in the driest period

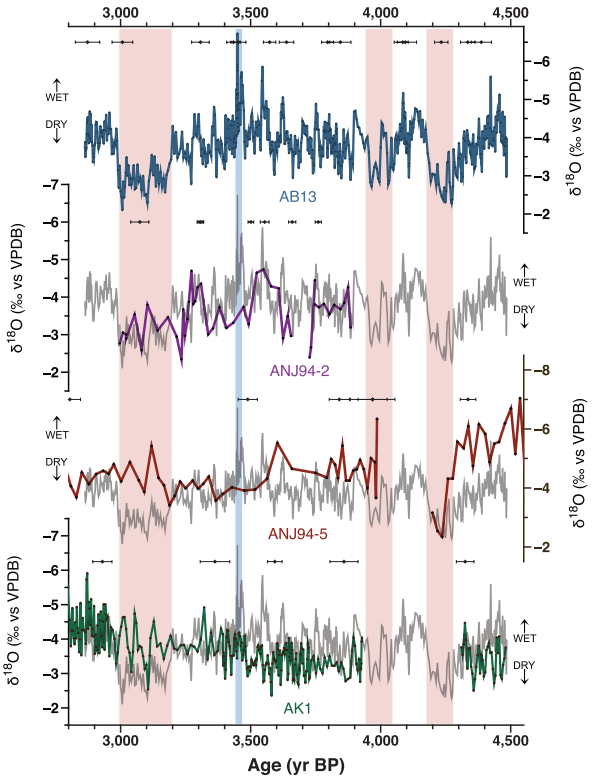

Figure 5. Comparison of northwestern Madagascar speleothem $\delta^{18}O$ records during the period of overlap with AB13. Highlighted bars indicate the wet interval (blue) and dry events (red) observed in AB13 record. From top: AB13 (this study), ANJ94-2 (Railsback et al. 2020), ANJ94-5 (Wang et al. 2019), and AK1 (Scroxton et al. 2023a). Previously published recordsare superimposed over AB13 $\delta^{18}O$ record (grey) and individual dates with error are shown above each record.

observed in this record, beginning at ~3120 y BP and lasting for about 200 years. To further assess the climatic signal in the region around Anjohibe, we compare our record with previously published mid-late Holocene records.

Comparison to previously published mid- to late-Holocene speleothems

Recent results from speleothems from across Madagascar have produced high resolution, well-dated paleoclimate reconstructions, with most of these studies using speleothems from Anjohibe (Burns et al., 2016; Duan et al., 2021; Voarintsoa et al., 2017, 2019; Wang et al., 2019) or from nearby Anjohikely (Scroxton et al., 2023a). The temporal coverage of several of these studies and our AB13 record partially overlap. One measure of the reliability of speleothem climate records is replication of the isotopic time series with other speleothems from the same approximate location (Dorale and Liu, 2009). In Figure 5 we compare our record to three previously published stalagmite records from NW Madagascar with varying temporal resolutions and dating accuracies: ANJ94-2 (Railsback et al., 2020) and ANJ94-5 (Wang et al., 2019) from Anjohibe and AK1 from Anjohikely ("little cave" in Malagasy), which is located 2.3 km southwest of Anjohibe (Scroxton et al., 2023a).

ANJ94-2 is both the shortest and lowest resolution, making it difficult to compare with AB13 in detail. $\delta^{18}O$ values generally fall within similar ranges across the two records. Both records follow similar climatic trends; slightly increasing precipitation from ~3885 to 3550 y BP and decreasing precipitation amounts from ~3325 to 3000 y BP (Figure 5). The record produced from stalagmite ANJ94-5 is also considerably lower resolution than that of AB13. However, both records broadly agree that from ~4455 to 4230 y BP, the climate above Anjohibe experienced relatively steady drying conditions (Figure 5). In ANJ94-5, this drying trend is followed by a growth hiatus, interpreted as the lack of deposition during intervals of significantly lower precipitation. The two early dry periods recorded in AB13 occurred within the time ANJ94-5 shows a growth hiatus, strengthening the argument that precipitation in the region was greatly reduced during this time. For the remainder of the record (from ~3985–2860 y BP), $\delta^{18}O$ values fall within a similar range as AB13, but no obvious trends occur in either record. The lack of simultaneous trends may be due to the large gap between dates in the upper portion of the ANJ94-5 record. which does not have dates between ~3487 and 2805 y BP. The potential for large changes in growth rates during this gap in ages makes a detailed comparison difficult for this period.

Comparison of AB13 with stalagmite AK1, the highest resolution of the three previously published records, shows similar decadal to centennial scale variability in oxygen isotopes throughout much of the record (Figure 5). AK1 exhibits a growth hiatus from ~4312 to 3929 y BP, further supporting the observed dry periods recorded in AB13 and ANJ94-5. From ~3310 to 2985 y BP, coincident with the drying trend and dry interval recorded in AB13, AK1 shows a period of slow growth followed by several positive isotope excursions. The structure and timing of these abrupt dry intervals is generally similar in both records. The lack of dates for AK1 during this >500-year interval may explain why the two records do not align more closely here.

Comparison of AB13 with these previously published speleothem records illustrates their broad agreement and reveals a coherent picture of the paleoclimate variability in the region. AB13 offers a more detailed record due to the higher temporal resolution and dating accuracy compared with ANJ94-5, AK1, and ANJ94-2. The interval of the 4.2 ka event appears to be dry in three records (with no information from ANJ94-2), as evidenced by less negative isotope values in AB13 and growth hiatuses in AK1 and ANJ94-5 (Figure 5). General increasing/decreasing precipitation trends and $\delta^{18}O$ value ranges are comparable across records.

Differences in the isotopic time series between AB13, AK1, ANJ94-5, and ANJ94-2 may largely be due to variation in sampling resolution and age models. It is also possible that variations in karst composition, drip-pathway, microbial ecosystem and/or overlying vegetation varied site to site may have resulted in slight variations in isotope values (Fairchild et al., 2006; Fohlmeister et al., 2020; Lachniet, 2009). Considering the variables, the records agree on a broad scale and even on a multi-centennial scale during the great majority of the period covered by AB13. We conclude that our results present a robust climate history for the region.

Hydroclimate variability in northwestern Madagascar during the 4.2 ka event

Scroxton et al. (2023a), referring to the 4.2 ka event, noted that, ". . .continually growing stalagmites are required to test the timing of the 4 kyr climate shift in the MSM [Malagasy Summer Monsoon] and synchronicity with wider Indian Ocean basin hydroclimate." Stalagmite AB13 provides such a record. Two previously published speleothem records from the study area, ANJ94-5 (Wang et al., 2019) and AK1 (Scroxton et al., 2023a), show increasing $\delta^{18}O$ values leading to hiatuses at or near the mid- to late- Holocene transition (~4300–3930 y BP). These hiatuses were interpreted as indicating dry conditions from about 4.3 ky BP to about 3.9 ky BP (Scroxton et al., 2023a; Wang et al., 2019; Figure 5). The sharp increases in $\delta^{18}O$ constructed from AB13 confirm previous interpretations of the growth hiatuses as dry periods. Scroxton et al. (2023a) compare AK1 with ANJ94-5

and suggests that although the onset and timing of the hiatuses in these two records fall within the age uncertainty of the 4.2 ka event, the drying trend preceding this anomaly was gradual and began at or before ~4500 y BP. The $\delta^{18}O$ record generated from AB13, also shows a gradual drying trend from ~4500 to 4300 y BP and it provides a detailed record of the rainfall variability across the gaps in previous records. Between ~4280 and 3950 y BP, Anjohibe experienced two distinct periods of drying. The first began at 4285 ± 45 y BP and ended at 4190 ± 45 y BP. After a wetter interval of abut 130 years, the second dry interval began at 4060 ± 55 y BP and ended at 3950 ± 55 y BP (Figure 3). The second dry interval is punctuated with wetter intervals and is not as dry as the first. The wet-dry-wet pattern of rainfall changes and the timing of the two dry intervals are within error of other high-resolution records from the broader Indian Ocean region. For example, Qunf Cave in southern Oman (Fleitmann et al., 2003) and Neor Lake in Iran both show two distinct dry intervals around 4.2 and 4.0 ky BP. Sahiya Cave in northern India (Kathayat et al., 2017) and a stalagmite record from northeastern Namibia (Railsback et al., 2018) also record a tripartite pattern, but in these records, the wet intervals around 4.2 ky BP and 4.0 ky BP are separated by a dry event. The areal extent of the 4.2 ka event and possible forcing mechanisms have been the subject of much debate (see e.g. Scroxton et al., 2023a and 2023b and references therein). Numerous mid- to late-Holocene transition records have shown climate anomalies around this time though more work is needed to establish the precise timing of the perturbation(s) and to determine if the records reflect one event or independent local/regional climate variability.

With regard to possible forcing, the 4.2 ka event has been attributed to a range of driving mechanisms including an influx of freshwater to the north Atlantic (Wang et al., 2013), a negative excursion in North Atlantic Oscillation (Yan and Liu, 2019), and the southern migration of the ITCZ (Railsback et al., 2018). Our Southern Hemisphere record of dry intervals associated with the 4.2 ka event is not consistent with a southward meridional migration of the tropical rain belt at that time. The 4.2 ka event may be unforced.

A complete record of the 4.2 ka event in Madagascar also helps to put the event into a broader climate perspective. Figure 3 shows that while the period from 3–9 ky BP to 4.2 ky BP has two distinct dry intervals, these are not the driest periods of the mid- to late-Holocene in northwest Madagascar. Oxygen isotopes suggest that the period from 4125 y BP to 3975 y BP was as dry or possibly slightly drier than the period from 4285 y BP to 4190 ± 45 y BP, while carbon isotopes suggest the younger of these intervals was considerably drier. The 4.2 ka event, then is not particularly remarkable as an "event" even in the fairly short time interval covered by the AB13 stalagmite.

Anjohibe and Rodrigues Island paleoclimate comparison

To determine if the climate variability we infer from Madagascar speleothem $\delta^{18}O$ extends to "nearby" Indian Ocean islands, we compared our record with others from Rodrigues Island. Li et al. (2020) presented a climate reconstruction of the last ~8000 years using speleothems collected from La Vierge cave located in southwest Rodrigues Island, which is ~1600 km east of Madagascar. Based on this isotope time series, records of modern precipitation, and model simulations, the authors suggest that on interannual to multidecadal scales, the hydroclimates of Rodrigues Island and Madagascar are comparable. They go on to infer possible relationships between "megadroughts" on Madagascar and the variations in the populations of large-bodied endemic vertebrates (megafauna) that went extinct in the Late-Holocene. The Rodrigues Island climate record has become a record of choice, taken as likely indicative of Madagascar's

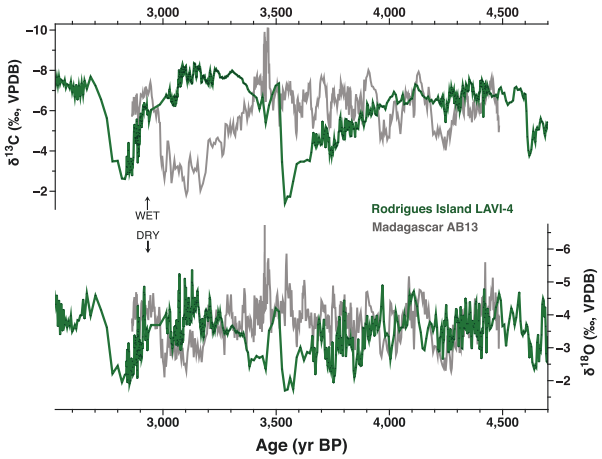

Figure 6. Comparison of Madagascar stalagmite sample AB13 and Rodrigues stalagmite sample LAVI-4 (Li et al. 2020) between (~2,664 – 4,507 years BP). Mean temporal resolution of AB13 ~2.7 years and LAVI-4 ~3.2 years.

climate history by other studies of Madagascar's megafaunal population dynamics (e.g. Broothaerts et al., 2023; Domic et al., 2021; Hansford et al., 2021; Hixon et al., 2021, 2022; Reinhardt et al., 2022).

Figure 6 presents a comparison between our AB13 paleoclimate record and the highest resolution speleothem record presented by Li et al. (2020), LAVI-4. From ~4480 to 4235 y BP, $\delta^{18}O$ values follow a similar drying trend with similarly timed decadal scale variability. However, after ~4200 y BP, the records become increasingly dissimilar and around 3780 y BP, the records diverge and often show an almost anti-phase relationship. For example, the most extensive droughts in LAVI-4, recorded at ~3650–3520 y BP, ~3460–3370 y BP and ~2870–2765 y BP do not match the driest periods in the compiled Anjohibe records and, in fact, coincide with the wettest periods recorded by AB13 (Figure 6). As Anjohibe became increasingly dry and entered into the longest dry period recorded by AB13, Rodrigues Island experienced the opposite, LAVI-4 shows the climate growing increasingly wet through this time. From 3945 to 4245 y BP where growth hiatuses occur in ANJ94-5 and AK1 and AB13 shows two periods of drying climate, LAVI-4 shows no extensive drought in Rodrigues.

The records also differ in terms of broad-scale trends. LAVI-4 shows an overall drying trend from ~ 4100 to 3540 y BP, whereas isotope values from AB13 indicate increasing precipitation during this time. From ~3150 to 2850 y BP, Rodrigues Island experienced another drying trend, while precipitation amounts at Anjohibe were increasing. The large number of dates for LAVI-4 during suggest excellent age control for the record, thus these differences are unlikely to be due to dating or temporal resolution.

Rodrigues Island and northwest Madagascar are likely responding to different climate forcings and/or local effects since they are climatologically distinct. As noted previously, Rodrigues Island lies directly in the easterly trade wind belt, while western Madagascar has a more complex relationship to summer easterlies (Li et al., 2021). Scroxton et al. (2017) suggested that northwest Madagascar may respond more to zonal climate variability associated with western Indian Ocean SSTs and the east to west tropical Indian Ocean sea surface temperature gradients than to meridional climate variability. Rodrigues Island is located sufficiently far to the east that it responds more to meridional climate variability associated with the location and intensity of the ITCZ than to zonal changes. Regardless of the cause, the periods of deepest drought in the LAVI-4 record do not match the periods of deepest drought in Madagascar, and the same is true for periods of

peak wetness (Figure 6). Thus, we suggest that speleothem records from Rodrigues Island should not be taken as indicative of paleoclimate variability in Madagascar.

Conclusions

Speleothem AB13 from Anjohibe cave in northwest Madagascar was used to produce a continuous, high-resolution, precisely dated record of hydroclimate variability in the region from ~4480 to ~2860 y BP. Oxygen and carbon stable isotopes and aragonite Sr/Ca provide three hydroclimate proxies that are in good agreement on hydroclimate change over the period of deposition. In addition, the AB13 records agree well with three additional speleothem $\delta^{18}O$ records from Anjohibe and nearby Anjohikely. The replication of the climate history from multiple proxies in AB13 and multiple speleothems strongly suggest that AB13 provides a robust, reliable climate history. The mechanism controlling Sr/Ca in the sample is initially the extent of prior calcite precipitation in the epikarst, a mechanism that has been suggested in numerous other studies. At ~4 ky BP, however, we interpret that the mechanism shifts to the degree of dolomite versus calcite dissolution in the epikarst. Three periods of relative drying, with peaks at ~4280–4230 y BP, ~4040–3960 y BP, and ~3180–2990 y BP occur. The wettest interval occurred from ~3470 to 3450 y BP and no long-term climate trend was apparent, although the record is relatively brief.

Our record includes continuous coverage of the 4.2 ka event in northwest Madagascar. Positive isotope excursions in both carbon and oxygen provide direct evidence of two distinct dry periods during ~4280 and 3950 years BP. That the 4.2 ka event is dry in Madagascar is supported by growth hiatuses from ~4200 y BP to 3800 y BP in two other speleothem records from Anjohibe. While clearly identifiable, the 4.2 ka event in northern Madagascar is not drier than other multi-decadal dry periods and is not the driest period in the AB13 record. With respect to possible forcing mechanisms of the 4.2 ka event, a southward shift in the mean position of the tropical rain associated with the ITCZ at 4.2 ky BP is not consistent with our record.

Our results differ significantly from a study of climate change during a similar time period on Rodrigues Island, 1800 km to the east. Thus, we suggest that climate records from Rodrigues Island should not be used to infer hydroclimate variability in Madagascar nor climate impacts on megafaunal population dynamics.

Acknowledgements

This research was conducted under a collaborative accord between the University of Massachusetts Amherst (Department of Anthropology, Department of Geoscience) and Université d'Antananarivo, Madagascar (Bassins sédimentaires, Evolution, Conservation). We are also grateful for the support and cooperation of the Ministère de la Communication et de la Culture for permission to conduct field work and recover and export samples, and to the Ministère auprès de la Présidence Chargé des Mines et du Pétrole, for permission to sample and export material to the U.S.A. We are grateful to William Clement for assistance with the spectral analyses.

Funding

The author(s) disclosed receipt of the following financial support for the research, authorship, and/or publication of this article: This research was supported by US National Science Foundation awards AGS-1702891/1702691, BCS-1750598 and EAR-1439559.

ORCID iDs

Berry L Williams https://orcid.org/0009-0001-2897-817X
Laurie R Godfrey https://orcid.org/0000-0001-9997-0207

Supplemental material

Supplemental material for this article is available online.

References

Araguás-Araguás L, Froehlich K and Rozanski K (2000) Deuterium and oxygen-18 isotope composition of precipitation and atmospheric moisture. *Hydrological Processes* 14(8): 1341–1355.

Barimalala R, Blamey RC, Desbiolles F et al. (2020) Variability in the Mozambique Channel trough and impacts on southeast African rainfall. *Journal of Climate* 33(2): 749–765.

Barimalala R, Desbiolles F, Blamey RC et al. (2018) Madagascar influence on the south Indian Ocean convergence zone, the Mozambique channel trough and southern African rainfall. *Geophysical Research Letters* 45(20): 11–380.

Bowen GJ, Cai Z, Fiorella RP et al. (2019) Isotopes in the water cycle: Regional- to global-scale patterns and applications. *Annual Review of Earth and Planetary Sciences* 47: 453–479.

Breitenbach SFM, Rehfeld K, Goswami B et al. (2012) Constructing proxy records from age models (COPRA). *Climate of the Past* 8(5): 1765–1779.

Brook GA, Rafter MA, Railsback LB et al. (1999) A high-resolution proxy record of rainfall and ENSO since AD 1550 from layering in stalagmites from Anjohibe Cave, Madagascar. *Holocene* 9(6): 695–705.

Broothaerts N, Razanamahandry VF, Brosens L et al. (2023) Vegetation changes and sediment dynamics in the Lake Alaotra region, central Madagascar. *Holocene* 33(4): 459–470.

Burney DA (1987) Late Holocene vegetational change in central Madagascar. *Quaternary Research* 28(1): 130–143.

Burney DA, Robinson GS and Burney LP (2003) *Sporormiella* and the late Holocene extinctions in Madagascar. *Proceedings of the National Academy of Sciences* 100(19): 10800–10805.

Burns SJ, Godfrey LR, Faina P et al. (2016) Rapid human-induced landscape transformation in Madagascar at the end of the first millennium of the Common Era. *Quaternary Science Reviews* 134: 92–99.

Cheng H, Fleitmann D, Edwards RL et al. (2009) Timing and structure of the 8.2 kyr BP event inferred from δ18O records of stalagmites from China, Oman, and Brazil. *Geology* 37(11): 1007–1010.

Cheng H, Lawrence Edwards R, Shen CC et al. (2013) Improvements in 230Th dating, 230Th and 234U half-life values, and U–Th isotopic measurements by multi-collector inductively coupled plasma mass spectrometry. *Earth and Planetary Science Letters* 371-372: 82–91.

Climate-data.org. Madagascar Climate: Average Temperature, Weather by Month, Madagascar Weather Averages. Available at: https://en.climate-data.org/africa/madagascar-177 (accessed 10 March 2023).

Dansgaard W (1964) Stable isotopes in precipitation. *Tellus A* 16(4): 436–468.

Dewar RE and Richard AF (2007) Evolution in the hypervariable environment of Madagascar. *Proceedings of the National Academy of Sciences* 104(34): 13723–13727.

Dietzel M, Gussone N and Eisenhauer A (2004) Co-precipitation of Sr2+ and Ba2+ with aragonite by membrane diffusion of CO2 between 10 and 50 °C. *Chemical Geology* 203(1-2): 139–151.

Domic AI, Hixon SW, Velez MI et al. (2021) Influence of late Holocene climate change and human land use on terrestrial and aquatic ecosystems in southwest Madagascar. *Frontiers in Ecology and Evolution* 9: 833.

Dorale JA and Liu Z (2009) Limitations of Hendy test criteria in judging the paleoclimatic suitability of speleothems and the need for replication. *Journal of Cave and Karst Studies* 71(1): 73–80.

Duan P, Li H, Sinha A et al. (2021) The timing and structure of the 8.2 ka event revealed through high-resolution speleothem records from northwestern Madagascar. *Quaternary Science Reviews* 268: 107104.

Fairchild IJ, Smith CL, Baker A et al. (2006) Modification and preservation of environmental signals in speleothems. *Earth-Science Reviews* 75(1-4): 105–153.

Fleitmann D, Burns SJ, Mudelsee M et al. (2003) Holocene forcing of the Indian monsoon recorded in a stalagmite from southern Oman. *Science* 300(5626): 1737–1739.

Fohlmeister J, Voarintsoa NRG, Lechleitner FA et al. (2020) Main controls on the stable carbon isotope composition of speleothems. *Geochimica et Cosmochimica Acta* 279: 67–87.

Gaetani GA and Cohen AL (2006) Element partitioning during precipitation of aragonite from seawater: A framework for understanding paleoproxies. *Geochimica et Cosmochimica Acta* 70(18): 4617–4634.

Gasse F and Van Campo E (1998) A 40,000-yr pollen and diatom record from Lake Tritrivakely, Madagascar, in the southern tropics. *Quaternary Research* 49(3): 299–311.

Gasse F and Van Campo E (2001) Late Quaternary environmental changes from a pollen and diatom record in the southern tropics (Lake Tritrivakely, Madagascar). *Palaeogeography Palaeoclimatology Palaeoecology* 167(3-4): 287–308.

Giri SJ, Swart PK and Devlin QB (2018) The Effect of changing seawater Ca and Mg concentrations upon the distribution coefficients of Mg and Sr in the skeletons of the scleractinian coral *Pocillopora damicornis*. *Geochimica et Cosmochimica Acta* 222: 535–549.

Gouhier TC, Grinsted A and Simko V (2021) R package biwavelet: Conduct Univariate and Bivariate Wavelet Analyses (version 0.20.19).

Gunn J (2004) *Encyclopedia of Caves and Karst Science*. Fitzroy Dearborn, New York.

Hansford JP, Lister AM, Weston EM et al. (2021) Simultaneous extinction of Madagascar's megaherbivores correlates with late Holocene human-caused landscape transformation. *Quaternary Science Reviews* 263: 106996.

Harvey CA, Rakotobe ZL, Rao NS et al. (2014) Extreme vulnerability of smallholder farmers to agricultural risks and climate change in Madagascar. *Philosophical Transactions of the Royal Society A*: 369(1639): 21030089.

Hersbach H, Bell B, Berrisford P et al. (2019) ERA5 monthly averaged data on single levels from 1979 to present. *Copernicus Climate Change Service (C3S) Climate Data Store (CDS)* 10: 252–266.

Hixon SW, Domic AI, Douglass KG et al. (2022) Cutmarked bone of drought-tolerant extinct megafauna deposited with traces of fire, human foraging, and introduced animals in SW Madagascar. *Scientific Reports* 12(1): 18504.

Hixon SW, Douglass KG, Crowley BE et al. (2021) Late Holocene spread of pastoralism coincides with endemic megafaunal extinction on Madagascar. *Proceedings of the Royal Society B* 288(1955): 20211204.

Jaffey AH, Flynn KF, Glendenin LE et al. (1971) Precision measurement of half-lives and specific activities ofU235andU238. *Physical Review C* 4(5): 1889–1906.

Jury MR (2003) The climate of Madagascar. In: Goodman SM and Benstead JP (eds) *The Natural History of Madagascar*. The University of Chicago Press, Chicago, pp.75–87.

Jury MR, Parker BA, Raholijao N et al. (1995) Variability of summer rainfall over Madagascar: Climatic determinants at interannual scales. *International Journal of Climatology* 15(12): 1323–1332.

Kathayat G, Cheng H, Sinha A et al. (2017) The Indian monsoon variability and civilization changes in the Indian subcontinent. *Science Advances* 3(12): e1701296.

Kinsman DJJ and Holland HD (1969) The co-precipitation of cations with CaCO3—IV. The co-precipitation of Sr2+ with aragonite between 16° and 96°C. *Geochimica et Cosmochimica Acta* 33(1): 1–17.

Konecky BL, Noone DC and Cobb KM (2019) The influence of competing hydroclimate processes on stable isotope ratios in tropical rainfall. *Geophysical Research Letters* 46(3): 1622–1633.

Koseki S and Bhatt BC (2018) Unique relationship between tropical rainfall and SST to the north of the Mozambique Channel in boreal winter. *International Journal of Climatology* 38: e378–e387.

Kurita N, Ichiyanagi K, Matsumoto J et al. (2009) The relationship between the isotopic content of precipitation and the precipitation amount in tropical regions. *Journal of Geochemical Exploration* 102(3): 113–122.

Lachniet MS (2009) Climatic and environmental controls on speleothem oxygen-isotope values. *Quaternary Science Reviews* 28(5-6): 412–432.

Li H, Cheng H, Sinha A et al. (2018) Hydro-climatic variability in the southwestern Indian Ocean between 6000 and 3000 years ago. *Climate of the Past* 14(12): 1881–1891.

Li H, Hu P, Zhang Q et al. (2021) Understanding interannual variations of the local rainy season over the southwest Indian Ocean. *Advances in Atmospheric Sciences* 38: 1852–1862.

Li H, Sinha A, Anquetil André A et al. (2020) A multimillennial climatic context for the megafaunal extinctions in Madagascar and Mascarene Islands. *Science Advances* 6(42): 2459.

Liu Y, San Liang X and Weisberg RH (2007) Rectification of the bias in the wavelet power spectrum. *Journal of Atmospheric and Oceanic Technology* 24(12): 2093–2102.

Madagascar (2020) LandLinks. Available at: https://www.landlinks.org/country-profile/madagascar/ (accessed 14 February 2023).

Marcott SA, Shakun JD, Clark PU et al. (2013) A reconstruction of regional and global temperature for the past 11,300 years. *Science* 339(6124): 1198–1201.

Matsumoto K and Burney DA (1994) Late Holocene environments at Lake Mitsinjo, northwestern Madagascar. *Holocene* 4(1): 16–24.

McDermott F (2004) Palaeo-climate reconstruction from stable isotope variations in speleothems: A review. *Quaternary Science Reviews* 23(7-8): 901–918.

Middleton J and Middleton V (2003) Karst and caves in Madagascar: Further observations. *Cave and Karst Science* 30: 125–128.

Mucci A, Canuel R and Zhong S (1989) The solubility of calcite and aragonite in sulfate-free seawater and the seeded growth kinetics and composition of the precipitates at 25°C. *Chemical Geology* 74(3-4): 309–320.

Railsback LB, Dupont LA, Liang F et al. (2020) Relationships between climate change, human environmental impact, and megafaunal extinction inferred from a 4000-year multi-proxy record from a stalagmite from northwestern Madagascar. *Quaternary Science Reviews* 234: 106244.

Railsback LB, Liang F, Brook GA et al. (2018) The timing, two-pulsed nature, and variable climatic expression of the 4.2 ka event: A review and new high-resolution stalagmite data from Namibia. *Quaternary Science Reviews* 186: 78–90.

Raveloson MLT, Newsome D, Golonka J et al. (2018) The contribution of Paleontology in the development of Geotourism in northwestern Madagascar: A preliminary assessment. *Geoheritage* 10: 731–738.

Reinhardt AL, Kasper T, Lochner M et al. (2022) Rain forest fragmentation and environmental dynamics of Nosy Be Island (NW Madagascar) at 1300 cal BP is attributable to intensified human impact. *Frontiers in Ecology and Evolution* 9: 1033.

Rogers RR, Hartman JH and Krause DW (2000) Stratigraphic analysis of Upper Cretaceous rocks in the Mahajanga Basin, northwestern Madagascar: Implications for ancient and modern faunas. *Journal of Geology* 108(3): 275–301.

Schott FA and McCreary JP (2001) The monsoon circulation of the Indian Ocean. *Progress in Oceanography* 51(1): 1–123.

Scroxton N, Burns S, Dawson P et al. (2018) Rapid measurement of strontium in speleothems using core-scanning micro X-ray fluorescence. *Chemical Geology* 487: 12–22.

Scroxton N, Burns SJ, McGee D et al. (2017) Hemispherically in-phase precipitation variability over the last 1700 years in a Madagascar speleothem record. *Quaternary Science Reviews* 164: 25–36.

Scroxton N, Burns SJ, McGee D et al. (2019) Competing temperature and atmospheric circulation effects on southwest Madagascan rainfall during the last deglaciation. *Paleoceanography and Paleoclimatology* 34(2): 275–286.

Scroxton N, Burns SJ, McGee D et al. (2023a) Hydroclimate variability in the Madagascar and Southeast African summer monsoons at the mid- to late-Holocene transition. *Quaternary Science Reviews* 300: 107874.

Scroxton N, Burns SJ, McGee D et al. (2023b) Tropical Indian Ocean basin hydroclimate at the mid- to late-Holocene transition and the double drying hypothesis. *Quaternary Science Reviews* 300: 107837.

Teixeira H, Montade V, Salmona J et al. (2021) Past environmental changes affected lemur population dynamics prior to human impact in Madagascar. *Communications Biology* 4(1): 1084.

Torrence C and Compo GP (1998) A practical guide to wavelet analysis. *Bulletin of the American Meteorological Society* 79: 61–78.

Vallet-Coulomb C, Gasse F, Robison L et al. (2006) Hydrological modeling of tropical closed Lake Ihotry (SW Madagascar): Sensitivity analysis and implications for paleohydrological reconstructions over the past 4000 years. *Journal of Hydrology* 331(1-2): 257–271.

Voarintsoa NR (2021) The Malagasy monsoon over the Holocene: A review from speleothem d18Oc records. *Malagasy Nature*.

Voarintsoa NRG, Matero ISO, Railsback LB et al. (2019) Investigating the 8.2 ka event in northwestern Madagascar: Insight from data–model comparisons. *Quaternary Science Reviews* 204: 172–186.

Voarintsoa NRG, Railsback LB, Brook GA et al. (2017) Three distinct Holocene intervals of stalagmite deposition and non-deposition revealed in NW Madagascar, and their paleoclimate implications. *Climate of the Past* 13(12): 1771–1790.

Voarintsoa NRG, Ratovonanahary ALJ, Rakotovao AZM et al. (2021) Understanding the linkage between regional climatology and cave geochemical parameters to calibrate speleothem proxies in Madagascar. *Science of the Total Environment* 784: 147–181.

Wang L, Brook GA, Burney DA et al. (2019) The African humid period, rapid climate change events, the timing of human colonization, and megafaunal extinctions in Madagascar during the Holocene: Evidence from a 2m Anjohibe Cave stalagmite. *Quaternary Science Reviews* 210: 136–153.

Wang S, Ge Q, Wang F et al. (2013) Abrupt climate changes of Holocene. *Chinese Geographical Science* 23: 1–12.

Wang YJ, Cheng H, Edwards RL et al. (2001) A high-resolution absolute-dated late pleistocene monsoon record from Hulu Cave, China. *Science* 294(5550): 2345–2348.

Wanner H, Mercolli L, Grosjean M et al. (2015) Holocene climate variability and change; a data-based review. *Journal of the Geological Society* 172(2): 254–263.

Wassenburg JA, Scholz D, Jochum KP et al. (2016) Determination of aragonite trace element distribution coefficients from speleothem calcite–aragonite transitions. *Geochimica et Cosmochimica Acta* 190: 347–367.

Yan M and Liu J (2019) Physical processes of cooling and megadrought during the 4.2 ka BP event: Results from TraCE-21ka simulations. *Climate of the Past* 15(1): 265–277.

Yoshimura K, Kanamitsu M, Noone D et al. (2008) Historical isotope simulation using reanalysis atmospheric data. *Journal of Geophysical Research Atmospheres* 113: D19108.

Zinke J, Dullo WC, Heiss GA et al. (2004) ENSO and Indian Ocean subtropical dipole variability is recorded in a coral record off southwest Madagascar for the period 1659 to 1995. *Earth and Planetary Science Letters* 228(1-2): 177–194.